Investigating Solidification and Liquation Cracking in Al 7075 Electron Beam Freeform Fabrication (EBF^3) Deposits

M. Cecilia Mulvaney[1], Marcia S. Domack[2], Karen M. B. Taminger[2], and James M. Fitz-Gerald[1]
[1] Department of Materials Science and Engineering, University of Virginia, Charlottesville, VA, USA, [2] NASA Langley Research Center, Hampton, VA, USA

National Aeronautics and Space Administration

Motivation

With a desire to increase production rates and reduce scrap, airframe companies are interested in high deposition rate additive manufacturing (AM) processes that are compatible with high-strength Al alloys for additive reinforcement of aircraft structures. The 7xxx-series Al-Zn-Mg-Cu alloys are of particular interest; however, these alloys exhibit severe hot cracking during welding and AM. While solutions to cracking have been developed for small-scale parts in powder-based AM processes through inoculation (Martin et al. 2017), no research has characterized the hot cracking behavior of 7xxx-series alloys with high deposition rate AM processes, such as electron beam freeform fabrication (EBF^3). Furthermore, there has been little effort to identify the underlying mechanisms of hot cracking in AM, with inoculant-based grain refinement used to suppress all hot cracking issues.

Lessons from welding show that a number of mechanisms can drive hot cracking, the most prominent being solidification cracking, which occurs in the fusion zone of a weld, and liquation cracking, which occurs outside of the fusion zone in the partially melted zone. Understanding the driving mechanisms is critical to more robust solutions to hot cracking in AM, particularly for high deposition rate processes, in which larger grains are inherent.

Hot Cracking: Welding and AM

- In welding, hot cracking is manifested in two primary forms (Kou 2003):
  - *Solidification cracking*, occurring interdendritically in the fusion zone (FZ), and
  - *Liquation cracking*, appearing intergranularly in the partially melted zone (PMZ) surrounding the FZ.
- Vaporization losses of alloying constituents such as Zn and Mg alter the FZ chemistry, potentially leading to greater hot cracking susceptibility.
- Current 7xxx-series Al AM literature reports intergranular hot cracks but does not distinguish between hot cracking mechanisms. Grain refinement by inoculation was found to circumvent cracking to enable powder-based AM of Al 7075 (Martin et al. 2017, Zhou et al. 2019).

(a) Regions of a fusion weld, including the fusion zone (FZ), partially melted zone (PMZ), heat affected zone (HAZ), and base metal (BM). (b) Vapor pressure vs. temperature curves for Al and the common 7xxx-series alloying elements (data replotted from Honig 1962).

EBF^3 of Al Alloys

- EBF^3 is a wire-based AM process developed at NASA in the early 2000's.
- Some Al alloys are compatible with EBF^3 but exhibit low strength (e.g. 2219).
- 7xxx-series alloys exhibit higher strength but are limited by weld hot cracking.

(a) EBF^3 chamber with wall deposits, (b) 2219 short deposit cross section, (c) dendritic top layer and (d) columnar middle layer microstructures.

References

Martin, J. *et al.* 3D printing of high-strength aluminum alloys. *Nature* 549: 365–369 (2017). Kou, S. Solidification and liquation cracking issues in welding. *JOM*, 55(6): 37-42, 2003. Zhou, L. *et al.* Microstructure and tensile property of a novel AlZnMgScZr alloy additively manufactured by gas atomization and laser powder bed fusion. *Scripta Materialia,* 158: 24-28, 2019. Honig, R. Vapor pressure data for the solid and liquid elements. *RCA Laboratories Review*, 23(4): 567-586, 1962. Borchers, T. *et al.* Aluminum alloy compositions, products and methods of making the same. *WO Patent 2018-157159 A1*: 210-220, 2018.

Objective

To understand hot cracking phenomena and driving mechanisms in Al 7075 EBF^3 deposits through characterization and comparison with those seen in welding to propose solutions for high deposition rate manufacturing of 7xxx-series Al alloys for additive reinforcement of aircraft structures.

EBF^3 Deposition Parameters

- Wall-shaped 4.1–7.4-cm tall x 1.3-cm wide deposits were printed with Al 7075 wire on 2.54-cm thick 7075 plate with 3.6 kW of power, a defocused and elliptically-rastered beam, 1.7 cm/s travel speed, 7.3 cm/s wire feed rate, 180º layer rotations, and pauses to control temperature.
- Substrate preheat temperature was varied between 170ºC and 320ºC.

Hot Cracking in 7075 EBF^3 Deposits

- X-ray computed tomography (XCT) scans revealed periodic 'macrocracks' transverse to the travel direction, with fine 'microcracks' appearing between macrocracks.
- Macrocracks were angled ~65º with respect to the plate and were oriented in opposing directions on the x-z deposit surfaces. Crack intervals were on the order of 1.2 - 1.8 cm.
- Fractography revealed that macrocrack surfaces were covered in dendrites, indicating the solidification cracking mechanism was in operation.
- Microcracks occurred below the topmost layer of the deposits and formed intergranularly between columnar grains, signaling the liquation cracking mechanism.

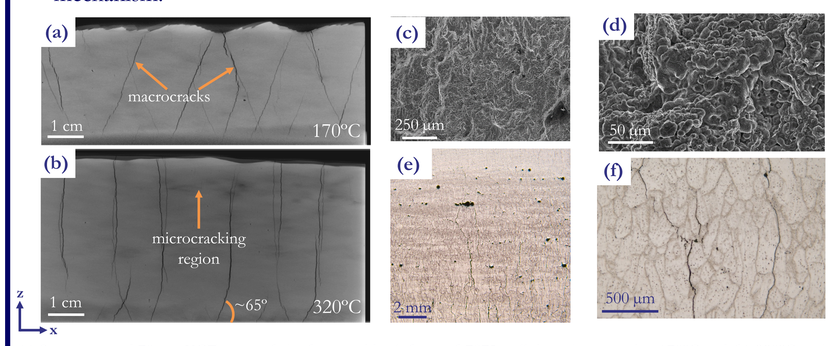

(a) Superimposed 70 µm XCT scans of the front and back faces of 7075 wall deposits printed at 170ºC and (b) 320ºC preheat temperatures, (c) SEM image of a typical macrocrack surface covered with dendrites, (d) close-up image of the dendrites, (e) typical etched microstructure with microcracks below the final layer, and (f) optical image of liquation microcracks.

Macrocrack Initiation and Propagation

- Macrocracks originate in the first and second layers of the deposits by the solidification cracking mechanism, since cracks occur in the FZ of the layer. The curved crack morphology denotes longitudinal and transverse constraints typical in a weld.
- Beginning with layer 3, cracks are straight and angled transverse to the travel direction, indicating a loss of transverse constraint and a shift to additive-type stresses.

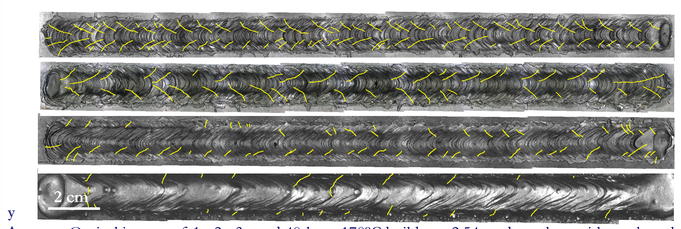

Layers	Crack density (cm^{-1})
1	1.9
2	1.1
3	0.67
40	0.36

Optical images of 1-, 2-, 3-, and 40-layer 170ºC builds on 2.54 cm baseplate, with cracks enhanced in yellow. 1- and 2-layer deposits exhibit curved cracks, while builds with more than 3 layers show shorter cracks at longer intervals.

Liquation Cracking vs. Preheat Temperature

- Microcracks stemmed from the root of the final layer in all deposits due to the liquation cracking mechanism.
- A 150ºC increase in the preheat temperature caused a 140% increase in liquation crack density and a 22% increase in average crack length due to deepening of the PMZ below each layer in the deposits.

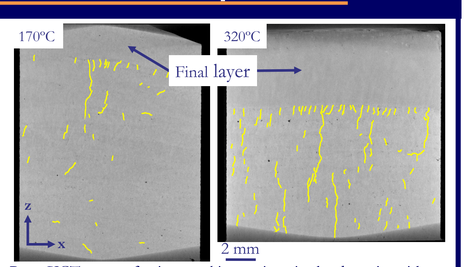

7 µm XCT scans of microcracking regions in the deposits with 170ºC and 320ºC preheat temperatures (cracks enhanced in yellow).

Hot Cracking Susceptibility Predictions

- The maximum steepness, $|dT/df_s^{1/2}|$, in the terminal stages of solidification in the Scheil plot is used as a solidification cracking susceptibility index (Kou 2015).
- The effect of vaporization losses of Zn and Mg in deposits of 7075 is reflected in the Scheil plot. Losses increased the cracking susceptibility index by 16-21%.
- Alloy X, a weld wire composition proposed by Borchers et al. in a 2018 patent, exhibits a susceptibility index 46% lower than that of Al 7075 due to additional Cu while retaining significant Zn and Mg for precipitation strengthening.
- Calculations for the readily weldable 2219 reveal an over 60% decrease in steepness.

Alloy	Zn	Mg	Cu	$\lvert dT/df_s^{1/2}\rvert$
7075[1]	5.70	2.42	1.52	4778
7075-A[2]	4.15	2.11	1.52	5581
7075-B[2]	3.67	1.97	1.52	5792
X[3]	2.9 - 3.4	1.4 - 1.9	4 - 4.5	2581
2219[1]	Mn: 0.22		6.38	1736

Alloy compositions (wt.%) and calculated $|dT/df_s^{1/2}|$ from Scheil solidification curves. A/B are the 170/320ºC preheated deposits.

[1] wire composition, [2] as-deposited composition, [3]Alloy X patent range.

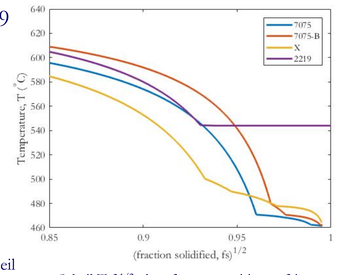

Scheil T-$f_s^{1/2}$ plots for compositions of interest.

Beam-Induced Grain Refinement

- Keyholing the rastered electron beam resulted in two vertical bands of equiaxed 38 µm grains, surrounded by 152 µm (area-averaged) diameter columnar grains.
- The refined grains accommodated solidification strains to suppress solidification macrocracking and resulted in a 4x reduction in liquation cracking density.

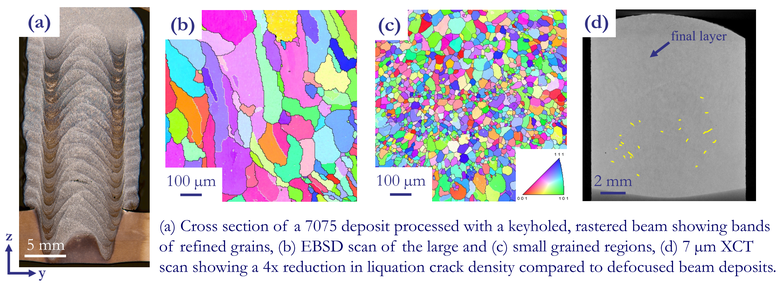

(a) Cross section of a 7075 deposit processed with a keyholed, rastered beam showing bands of refined grains, (b) EBSD scan of the large and (c) small grained regions, (d) 7 µm XCT scan showing a 4x reduction in liquation crack density compared to defocused beam deposits.

Conclusions

- Large macrocracks formed in the first layer of the deposits by the solidification cracking mechanism and propagated through the height, changing orientation as the stress state transitioned from that of welding to additive manufacturing.
- Fine microcracks below the final layer of the deposits were formed by the liquation cracking mechanism. Increasing the preheat temperature resulted in a larger PMZ, causing a 140% higher liquation crack density and 22% longer cracks.
- Vaporization losses of Zn and Mg increased hot cracking susceptibility by 20%.
- Compositional design of alloys with lower susceptibility to cracking coupled with inoculant- or beam-induced grain refinement will enable EBF^3 of Al 7075.

Future Work

- Use Scheil analysis to design wire feedstock compositions that reduce the inherent solidification cracking susceptibility while retaining significant amounts of Zn and Mg for precipitation strengthening.
- Pursue trace Zr additions to feedstock wire for inoculating refined grains.
- Explore other beam-induced grain refining techniques on full-scale deposits, including beam current and/or wire pulsation.

Acknowledgements

This work was funded by the NASA Advanced Air Transportation Technology (AATT) project. Special thanks to the Advanced Materials and Processing Branch and technicians at NASA Langley for their support.